Statistica Sinica Preprint No: SS-2020-0118	
Title	Bayesian Estimation of Gaussian Conditional Random Fields
Manuscript ID	SS-2020-0118
URL	http://www.stat.sinica.edu.tw/statistica/
DOI	10.5705/ss.202020.0118
Complete List of Authors	Lingrui Gan, Naveen Narisetty and Feng Liang
Corresponding Author	Naveen Narisetty
E-mail	naveen@illinois.edu
Notice: Accepted version subject to English editing.	

Bayesian Estimation of Gaussian Conditional Random Fields

Lingrui Gan, Naveen N. Narisetty, and Feng Liang

Department of Statistics, University of Illinois at Urbana-Champaign

Abstract: We propose a novel methodology based on a Bayesian Gaussian conditional random field model for elegantly learning conditional dependence structures among multiple outcomes, and between the outcomes and a set of covariates simultaneously. Our approach is based on a Bayesian hierarchical model using a spike and slab Lasso prior. We investigate the corresponding maximum a posterior (MAP) estimator that requires dealing with a non-convex optimization problem. In spite of the non-convexity, we establish statistical accuracy for all points in the high posterior region including the MAP estimator and propose an efficient EM algorithm for computation. Through simulation studies and a real application, we demonstrate the competitive performance of our method for the purpose of learning the dependence structure.

Key words and phrases: Gaussian conditional random field; Spike and slab Lasso prior; Bayesian regularization; Graphical models.

1. Introduction

Graphical models are widely used in applications where the key interest is to identify the conditional dependence structure among a set of variables $Y = (Y^{(1)}, ..., Y^{(p)}) \in \mathbb{R}^p$. A special class of graphical models is the Gaussian graphical model, under which Y follows a multivariate Gaussian distribution with mean zero and precision matrix Θ. Estimating the underlying dependence structure of a Gaussian graphical model (GGM) is equivalent to estimating Θ, because of a well-known fact that the (i, j)-th element of Θ being zero is equivalent to conditional independence of $Y^{(i)}$ and $Y^{(j)}$ given the other variables. Due to this connection, sparse precision matrix estimation is an important and well-studied research problem (Meinshausen and Bühlmann, 2006; Banerjee et al., 2008; Friedman et al., 2008; Rothman et al., 2010; Ravikumar et al., 2011; Gan et al., 2019).

In many application contexts, a marginal Gaussian graphical model for the outcomes alone is not sufficient and it is important to take covariate information into consideration. For example, in the analysis of gene expression data, it is of interest to model genetic outcomes given biomarker information, or in the context of portfolio analysis, it is of interest to model asset prices given historical pricing information. In such applications, along with understanding the dependence relationship among the many outcome

variables Y, it is also important to study the relationship between Y and the covariates $X = (X^{(1)}, ..., X^{(q)}) \in \mathbb{R}^q$. While one can model (Y, X) jointly using a GGM and obtain the conditional relationship between Y's, and between X's and Y's as a partial product of the model, it is redundant to model the dependence structure among the X's which leads to inefficiency when $q \gg p$. We discuss this issue in Section 2.

To learn the conditional dependence structures between outcomes, and between outcomes and covariates, Gaussian conditional random field (GCRF) model has been recently considered (Sohn and Kim, 2012; Yuan and Zhang, 2014; Wytock and Kolter, 2013). The GCRF model provides a more suitable and precise description of the desired conditional dependence structure compared to modeling the entire Gaussian graphical model on both X and Y or modeling only the dependence structure among Y by eliminating the effects of X through a multivariate regression model (Cai et al., 2012; Rothman et al., 2010; Yin and Li, 2011; Deshpande et al., 2017). Estimation methods based on ℓ_1 penalization for the GCRF model have been proposed and their theoretical properties for estimation accuracy have been studied by Wytock and Kolter (2013) and Yuan and Zhang (2014). GCRF estimation using ℓ_1 penalization for latent X is recently studied by Frot et al. (2019). Although ℓ_1-penalty encourages sparsity while being convex, it has

some well-known limitations, such as the bias it induces for large parameter values (Fan and Li, 2001; Lam and Fan, 2009; Zhang, 2010; Zhang and Zhang, 2012; Loh and Wainwright, 2017). Moreover, the theoretical results for structure recovery of ℓ_1 penalization based GCRF require restrictive mutual incoherence conditions (Wytock and Kolter, 2013). In this paper, we provide an alternative framework for estimation of the Gaussian conditional random field model using a Bayesian framework with spike and slab Lasso priors (Ročková, 2018; Ročková and George, 2018). The maximum a posteriori (MAP) estimator can be viewed as a penalized likelihood estimator with a non-convex penalty function induced from the spike and slab Lasso prior, which has been recently studied to have good regularization properties in the contexts of linear regression (Ročková, 2018; Ročková and George, 2018) and Gaussian graphical models (Gan et al., 2019).

We address novel theoretical and computational challenges posed by the GCRF model under the Bayesian setting. The likelihood corresponding to GCRF need not satisfy the restricted strong convexity property (Loh and Wainwright, 2017) and the Bayesian penalty function corresponding the spike and slab Lasso prior need not have bounded second derivative at all the parameter values; all these pose new challenges for studying the properties of our MAP estimator. For example, without such properties,

local optima may not be unique and general results from existing work (Loh and Wainwright, 2017) on support recovery for non-convex optimization are not applicable. Despite the challenges imposed by both the likelihood and the non-convexity, we show that all points from the high posterior density (HPD) region including the MAP estimator have an optimal convergence rate in Frobenius norm, and there exists at least one local optimum that converges in ℓ_∞ norm and achieves the support recovery consistency, without the incoherence condition required by Wytock and Kolter (2013). We also show that the optimal converge rate in ℓ_∞ norm holds for all local modes of the fractional posterior, i.e., posterior that is defined with respect to a fractional likelihood. Our theoretical results (presented in Section 3) are stronger than the ones on the Gaussian conditional random field model with ℓ_1 penalty from Yuan and Zhang (2014) and Wytock and Kolter (2013), and more generally provide novel contributions to the theoretical properties of non-convex penalization in the spirit of Fan and Li (2001); Lam and Fan (2009); Negahban et al. (2009); Zhang (2010); Zhang and Zhang (2012); Loh and Wainwright (2015, 2017).

We propose an efficient EM algorithm for computation (described in the Supplementary Material) which has the same computational complexity as the state-of-the-art optimization algorithm for the Gaussian conditional

random field with ℓ_1 penalty (Wytock and Kolter, 2013; Yuan and Zhang, 2014). Our empirical studies in Section 4 demonstrate that the proposed Bayesian regularization approach provides a competitive performance compared to alternative methods both for estimation and structure recovery.

2. Bayesian regularization for Gaussian conditional random fields

2.1 Model formulation

Consider a p-dimensional outcome Y and a q-dimensional covariate X. As an analog to the conditional random field for discrete variables proposed by Lafferty et al. (2001), Gaussian conditional random field model (Sohn and Kim, 2012; Yuan and Zhang, 2014; Wytock and Kolter, 2013) assumes the conditional density function of Y given X as:

$$p(Y \mid X, \Lambda, \Theta) \propto \sqrt{\det(\Lambda)} \exp\left\{-\frac{1}{2} Y^T \Lambda Y - X^T \Theta Y\right\}, \qquad (2.1)$$

where Λ is a $p \times p$ positive definite and symmetric matrix and $\Theta \in \mathbb{R}^{q \times p}$ is a matrix of dimension $q \times p$. Throughout, we use Φ as a compact notation for parameters Λ and Θ. Given a set of n random samples $(X_i, Y_i)_{i=1}^n$, the corresponding log-likelihood function is given by

$$\ell(\Phi) = \frac{n}{2}\Big(\log\det(\Lambda) - \mathrm{tr}(S_{yy}\Lambda + 2S_{xy}\Theta + \Lambda^{-1}\Theta^T S_{xx}\Theta)\Big), \qquad (2.2)$$

where $S_{yy} = \frac{1}{n}\sum_{i=1}^{n} Y_i Y_i^T$, $S_{xy} = \frac{1}{n}\sum_{i=1}^{n} X_i^T Y_i$, $S_{xx} = \frac{1}{n}\sum_{i=1}^{n} X_i X_i^T$, and the constant terms not involving the parameters are omitted. Irrelevant to the marginal distribution of X, the sparsity patterns of Φ determine the conditional dependence relationship between the components of Y and the dependence between X and Y:

$$\Theta_{ij} = 0 \quad \Longleftrightarrow \quad X^{(i)} \perp\!\!\!\perp Y^{(j)} \mid X^{-(i)}, Y^{-(j)},$$
$$\Lambda_{ij} = 0 \quad \Longleftrightarrow \quad Y^{(i)} \perp\!\!\!\perp Y^{(j)} \mid X, Y^{-(i,j)},$$

where $\perp\!\!\!\perp$ denotes independence. Moreover, the GCRF model avoids modeling the dependence structure among the X's which is beneficial both computationally and theoretically when the dimension of X is large. We now discuss two alternative modeling frameworks which produce some descriptions of the conditional dependence structure.

2.1.1 Joint Gaussian graphical model on (X, Y)

One common approach used for learning the dependence structure is to model (X, Y) using a joint graphical model. With the additional assumption that X is normally distributed with mean zero, the Gaussian conditional random field model implies that (X, Y) jointly follows a multivariate

Gaussian distribution:

$$\begin{pmatrix} X \\ Y \end{pmatrix} \sim N\left(\mathbf{0}, \begin{bmatrix} \Omega_{xx} & \Theta \\ \Theta^T & \Lambda \end{bmatrix}^{-1}\right). \tag{2.3}$$

Therefore Θ and Λ can be obtained as a partial outcome from fitting a large Gaussian graphical model jointly on (X, Y) using existing algorithms on high-dimensional Gaussian graphical models such as the graphical Lasso as done by Witten and Tibshirani (2009).

This approach, however, is not optimal if we are only interested in Θ and Λ. When the dimension of X is much larger than the dimension of Y, the computational cost is dominated by estimating the graphical structure of X, which is not of our interest. Theoretically, the error from estimating Ω_{xx} may affect the estimation accuracy in estimating Θ and Λ, since the accuracy is affected by the degree of sparsity of the entire graph (Bickel and Levina, 2008; Cai et al., 2011; Ravikumar et al., 2011; Loh and Wainwright, 2015, 2017; Gan et al., 2019). To avoid estimating the irrelevant structure among the X variables, one could work with the profile likelihood,

$$\tilde{\ell}(\Phi) = \max_{\Omega_{xx}} \tilde{\ell}(\Omega_{xx}, \Theta, \Lambda),$$

where $\tilde{\ell}(\Omega_{xx}, \Theta, \Lambda) = \log \prod_{i=1}^{n} p(X_i, Y_i \mid \Omega_{xx}, \Theta, \Lambda)$ is the log-likelihood of the joint Gaussian distribution (2.3). As shown by Yuan and Zhang (2014),

the profile likelihood $\tilde{\ell}(\Phi)$ is exactly equal to the Gaussian conditional random field likelihood defined by (2.2). Although it can be viewed as the profile likelihood of a joint Gaussian graphical model on (X, Y), our Gaussian conditional random field model makes no assumption on the marginal distribution of X and is even applicable when X is discrete.

2.1.2 Covariate-adjusted graphical model

The other alternative modeling framework that can be used to learn the conditional dependence structure is the multivariate regression framework. The conditional distribution of Y given X due to the Gaussian conditional random field model (2.1) can be reparametrized as a multivariate regression model with B as the regression coefficient matrix and Λ as the error precision matrix as follows:

$$Y \mid X \sim N(BX, \Lambda^{-1}), \quad B = -\Lambda^{-1}\Theta^T. \tag{2.4}$$

Within this regression framework, which is often referred to the covariate-adjusted graphical model, several approaches have been proposed to estimate B and Λ under sparsity assumptions on them (Cai et al., 2012; Rothman et al., 2010; Yin and Li, 2011; Deshpande et al., 2017).

Although Λ indeed reveals the conditional dependence structure among the elements of Y, the sparsity pattern of B is different from the sparsity

pattern of Θ. The regression coefficients B_{ij} indicate how the conditional mean $\mathbb{E}(Y^{(i)}|X)$ depends on the X variables without conditioning on the other Y variables, while Θ_{ij} reflects the conditional dependence between $Y^{(i)}$ and $X^{(j)}$ given all the other X and Y variables. Apart from the differences in the sparsity structures, another major difference between the two parameterizations is that the log-likelihood function of the Gaussian conditional random field parameterized by (Θ, Λ) is convex, while the one from the multivariate regression parameterized by (B, Λ) is not convex (Yuan and Zhang, 2014).

2.2 Proposed Bayesian regularization formulation

Our goal is to estimate the parameters Θ and Λ for the GCRF model (2.1) under the assumption of sparsity. Although ℓ_1 regularization is a natural choice as considered by Yuan and Zhang (2014) and Wytock and Kolter (2013) for the GCRF model, this approach induces bias on the parameters with large values and also requires strong mutual incoherence assumptions for consistently achieving graph structure recovery. This motivates our work to consider an alternative formulation from the Bayesian regularization framework due to its promising performance in recent work (Ročková and George, 2016, 2018; Gan et al., 2019).

We consider the spike and slab Lasso prior which takes the form of a mixture of two Laplace distributions:

$$\pi_{\text{SS}}(\theta) = \eta \cdot \text{LP}(\theta; v_1) + (1-\eta) \cdot \text{LP}(\theta; v_0), \tag{2.5}$$

where $\text{LP}(\theta; v) = 1/(2v)e^{-|\theta|/v}$ denotes the density function of a Laplace distribution with scale parameter v, the two scale parameters satisfy $v_1 > v_0 > 0$, and η is the mixing weight. Spike and slab priors with Gaussian components have long been used for Bayesian variable selection (George and McCulloch, 1993; Ishwaran and Rao, 2005; Narisetty and He, 2014) and more recently the spike and slab Lasso prior has been demonstrated to yield desirable shrinkage properties for sparse estimation (Ročková and George, 2014; Ročková, 2018; Ročková and George, 2018; Gan et al., 2019).

The following alternative representation of the spike and slab Lasso prior (2.5) may help to explain the motivation behind such a mixture representation:

$$\pi(\theta|\gamma) = \text{LP}(\theta; v_1)^{\gamma} \cdot \text{LP}(\theta; v_0)^{(1-\gamma)}, \qquad \gamma \sim \mathsf{Bern}(\eta),$$

where the binary variable γ can be interpreted as the indicator for the θ being signal or noise. When $\gamma = 1$, the unknown parameter θ is expected to represent signal taking a relatively large value and is modeled by a Laplace distribution with a larger scale parameter v_1 (i.e., the "slab" component);

when $\gamma = 0$, the unknown parameter θ is expected to represent noise taking a value close to zero and is modeled by a Laplace distribution with a small scale parameter v_0 (i.e., the "spike" component).

We place the spike and slab Lasso prior on all the entries of Θ and the upper triangular entries of Λ (due to symmetry), and place a Uniform prior on the diagonal entries of Λ:

$$\pi(\Phi) = \Big[\prod_{i,j} \pi_{\text{SS}}(\Theta_{ij})\Big] \times \Big[\prod_{i<j} \pi_{\text{SS}}(\Lambda_{ij})\Big] \times \Big[\prod_{i} \pi_{\text{Unif}}(\Lambda_{ii})\Big].$$

The support of the joint prior distribution is the set $\{(\Theta, \Lambda) : \Lambda \succ 0, \|\Lambda\|_2 \leq R\}$, where $\Lambda \succ 0$ means that Λ is positive definite. We constrain the matrix L_2 norm of Λ to be upper bounded. Although this additional side constraint adds a restriction to the high-dimensional parameter space, it is not so restrictive as the upper bound R is allowed to change with (n, p, q) and can be quite large.

2.3 MAP estimator: a penalized likelihood perspective

For computational efficiency, we estimate (Θ, Λ) using the posterior mode. The negative log posterior can be written as

$$L(\Phi) = -\ell(\Phi) + \sum_{i,j} \text{pen}_{\text{SS}}(\Theta_{ij}) + \sum_{i<j} \text{pen}_{\text{SS}}(\Lambda_{ij}), \tag{2.6}$$

where $\ell(\cdot)$ is the log-likelihood function (2.2) and $\text{pen}_{\text{SS}}(\cdot)$ is the negative logarithm of the spike and slab Lasso prior (2.5):

$$\text{pen}_{\text{SS}}(\theta) = -\log\Big(\frac{\eta}{2v_1}e^{-\frac{|\theta|}{v_1}} + \frac{1-\eta}{2v_0}e^{-\frac{|\theta|}{v_0}}\Big). \tag{2.7}$$

Finding the MAP estimator of (Θ, Λ) is equivalent to solving the optimization problem

$$\underset{\Theta,\Lambda\succ 0, \|\Lambda\|_2 \le R}{\arg\min} \; L(\Phi). \tag{2.8}$$

The minimizer of (2.6) has a natural interpretation as the penalized likelihood estimator using the penalty function (2.7) which is induced by the Bayesian spike and slab Lasso prior. In the penalized likelihood framework, the derivative of a penalty function $\text{pen}'_{\text{SS}}(\theta)$ often plays the role of thresholding. An ideal property of a penalty function is to threshold adaptively: $\text{pen}'_{\text{SS}}(\theta)$ is large when θ is small so the resulting estimate will be exactly zero, and $\text{pen}'_{\text{SS}}(\theta)$ is small when θ is large so the resulting estimate is almost unbiased without being affected by the thresholding value. It is well-known that the Bayesian penalty induced from a single Laplace prior $\text{LP}(\theta; v)$ is equivalent to the ℓ_1 penalty (Tibshirani, 1996; Park and Casella, 2008), whose derivative takes a constant value and therefore does not possess such an adaptive property, which is particularly helpful for achieving structure recovery properties.

In the Proposition below, which is a generalization of the Lemma 1 of Ročková and George (2018), we show that the first and the second derivatives of our Bayesian penalty function, induced by the spike and slab Lasso prior, can be linked to the mean and variance of a family of binary random variables.

Proposition 1. *$pen_{SS}(\theta)$ is a concave function when θ in $\mathbb{R}^+$, with*

$$\begin{aligned} pen'_{SS}(\theta) &= \mathbb{E}Z(\theta) = \frac{\eta(\theta)}{v_1} + \frac{1-\eta(\theta)}{v_0}, \\ pen''_{SS}(\theta) &= -Var(Z(\theta)) = \eta(\theta)(1-\eta(\theta))\left(\frac{1}{v_0} - \frac{1}{v_1}\right)^2, \end{aligned}$$

where $Z(\theta)$ is a binary random variable taking the value $1/v_1$ with probability $\eta(\theta)$, and the value $1/v_0$ with probability $1-\eta(\theta)$ where $\eta(\theta)$ is given by $\eta(\theta) = \frac{\eta LP(\theta;v_1)}{\eta LP(\theta;v_1)+(1-\eta)LP(\theta;v_0)}$.

A consequence of Proposition 1 is that the spike and slab Lasso prior leads to an adaptive regularization procedure: $\text{pen}'_{\text{SS}}(\theta)$ is a decreasing function with respect to the magnitude of θ. In particular, the penalty at θ is a weighted average of a large penalty $1/v_0$ and a small one $1/v_1$ where the weights $\eta(\theta)$ and $1-\eta(\theta)$ are the conditional probabilities of θ belonging to the "slab" or the "spike" component, respectively.

3. Theoretical results

For our theoretical studies, we evaluate the performance of our Bayesian procedure under the frequentist data generating mechanism, that is, under the assumption that the data Y are generated based on a fixed set of parameters Φ^0. This is a common practice for theoretical analysis of Bayesian methods such as the analyses in Ishwaran and Rao (2005); Narisetty and He (2014); Castillo et al. (2015); Gan et al. (2019).

We first provide optimal ℓ_2 error bounds for all points from the high posterior density (HPD) region:

$$\begin{aligned} \text{HPD} &= \{\Phi : \pi(\Phi \mid \text{Data}) \geq \pi(\Phi^0 \mid \text{Data})\} \\ &= \{\Phi : L(\Phi) \leq L(\Phi^0)\}, \end{aligned} \tag{3.9}$$

and show that there exists at least one local optimum in HPD that has the optimal error rate in ℓ_∞ norm and that it has the same support as the true graph. We further show that the optimal error rate in ℓ_∞ norm holds for all local modes of the fractional posterior, i.e., posterior that is defined with respect to a fractional likelihood.

Our results on optimal error rate in ℓ_∞ norm lead to support recovery consistency, without the incoherence condition required by Wytock and Kolter (2013). We would like to note that some of the existing works also

do not require the incoherence condition but there are important distinctions of our results. The results for SCAD in Fan and Li (2001) are valid only for one of the local solutions whereas our results ascertain the consistency for all solutions. The results of Cai et al. (2011) are applicable only to the unconditional graphical models and are not directly applicable to the setting with covariates using Gaussian conditional random field model (GCRF), which is quite different from unconditional graphical models.

Notation. Denote the true parameters to be Φ^0, Λ^0, and Θ^0, respectively. Let $S_0 = \{(i,j) : \Phi^0_{ij} \neq 0\}$ denote the signal set, $\theta^0_{\min} = \max_{(i,j)\in S_0} |\Phi^0_{ij}|$ the minimal signal strength, and $d = \max_{i=1:(p+q)} \mathrm{card}\{j : \Phi^0_{ij} \neq 0\}$ the maximum degree of the underlying conditional graph. We use $\lambda_{\min}(A)$ and $\lambda_{\max}(A)$ to denote the largest and smallest eigenvalues of a symmetric matrix A, respectively, and $|||\cdot|||_\infty$ to denote ℓ_∞/ℓ_∞ operator norm of a matrix. Define

$$c_{\Theta^0} = |||(\Theta^0)^T|||_\infty, \quad c_{\Lambda^0} = |||(\Lambda^0)^{-1}|||_\infty, \quad c_H = \frac{n}{2}|||H^{-1}_{S_0S_0}|||_\infty,$$

where $H := \nabla^2\ell(\Phi^0)$ denotes the Hessian matrix evaluated at Φ^0, and $H^{-1}_{S_0S_0}$ denotes a submatrix of H^{-1} with row and column indices from set S_0. Note that H is a matrix with dimension equal to the number of total parameters in Φ. Further define $K_* = 8\max_i \Sigma^0_{ii} + 8\max_i \left((\Lambda^0)^{-1}\Theta^T\Sigma^0_{xx}\Theta(\Lambda^0)^{-1}\right)_{ii}$,

where Σ^0 denotes the covariance matrix of (X, Y) and Σ^0_{xx} the covariance matrix of X.

We would like to emphasize that the symbols used in our theorems and proofs do not represent fixed constants and may vary with n, unless otherwise specified. We basically drop the subscript n from symbols, otherwise we would write $p = p_n$, $\Phi^0 = \Phi^0_n$; our notation is similar to the one used in Loh and Wainwright (2017). In particular, this implies that the minimum and maximum nonzero entries of the true parameters can depend on the sample size. Note that K_* is upper bounded by the maximum variance of all the variables and so K_* can be upper bounded by a fixed constant not depending on n if the the variances of all the covariates and the response variables are upper bounded.

3.1 Some preliminary results

Before presenting our results, we first present some preliminary results from the literature on the log-likelihood function $\ell(\Phi)$.

In our analysis, we will examine $\ell(\Phi)$ in a small neighborhood around the true parameter value Φ^0. Expand $\nabla\ell(\Phi^0 + \Delta)$ as follows:

$$\nabla\ell(\Phi^0) + H \cdot \mathrm{vec}(\Delta) + R(\Delta) \tag{3.10}$$

where $H = \nabla^2\ell(\Phi^0)$ is the Hessian matrix and $R(\Delta) = \nabla\ell(\Phi^0 + \Delta) -$

$\nabla\ell(\Phi^0) - H \cdot \mathrm{vec}(\Delta)$ denotes the residual. The following Lemma provides some useful bounds for $\nabla\ell(\Phi^0)$ and $R(\Delta)$. We omit the proof here, since the first bound is the same as Proposition 4 in Yuan and Zhang (2014) and the second bound is similar to Lemma 3 in Wytock and Kolter (2013) with their notation of $\|S_{xx}\|_\infty \leq c_X^2$ replaced by $\|S_{xx}\|_\infty \leq 9\rho_2$, where where $\rho_2 = 1.5\lambda_{\max}(\Sigma^0_{xx})$. Note that our log-likelihood function $\ell(\Phi)$ differs from theirs by a factor $n/2$.

Lemma 1. *Assume data are generated from a GCRF model with true parameter* Φ^0.

1. *We have* $\|\nabla\ell(\Phi^0)\|_\infty \leq K_*\sqrt{n\log(10(p+q)^2/\eta)}$ *with probability* $1-\epsilon_0$ *given the sample size* $n \geq \log(10(p+q)^2/\epsilon_0)$, *where* ϵ_0 *is any constant in* $(0,1)$.

2. *If* $\|\Delta\|_\infty \leq \frac{1}{d}\min\{\frac{1}{3c^0_\Lambda}, \frac{c_{\Theta^0}}{2}\}$, *then* $\frac{2}{n}\|R(\Delta)\|_\infty \leq 1854d^2c^2_{\Theta^0}c^4_{\Lambda^0}\rho_2\|\Delta\|_\infty$, *where* $\rho_2 = 1.5\lambda_{\max}(\Sigma^0_{xx})$.

Local strong convexity of the log-likelihood function $\ell(\Phi)$ plays an important role in our theoretical analysis. Following Yuan and Zhang (2014), we define the local restricted strong convexity (LRSC) constant, a quantity

that measures the local curvature of $\ell(\Phi)$ at Φ^0:

$$\beta(\Phi^0; r, \alpha) = \inf \left\{ \frac{\langle \nabla \ell(\Phi^0 + \Delta) - \nabla \ell(\Phi^0), \Delta \rangle}{\|\Delta\|_2^2} \quad : \quad \|\Delta\|_2 \leq r, \right.$$
$$\left. \|\Delta_{S_0^c}\|_1 \leq \alpha \|\Delta_{S_0}\|_1 \right\}.$$

We next state an assumption that is needed in our theoretical analysis.

Assumption 1: Assume that the covariate vector X is from a random design with covariance matrix Σ_{xx}^0 and satisfies the following s_0-sparse restricted isometry property condition:

$$\begin{cases} \inf \left(\frac{u^T S_{xx} u}{u^T \Sigma_{xx}^0 u} : u \neq 0, \|u\|_0 \leq s_0 \right) \geq 0.5, \\ \sup \left(\frac{u^T S_{xx} u}{u^T \Sigma_{xx}^0 u} : u \neq 0, \|u\|_0 \leq s_0 \right) \leq 1.5, \\ \frac{\lambda_{\max}[(\Theta^0)^T S_{xx} \Theta^0]}{\lambda_{\max}[(\Theta^0)^T \Sigma_{xx}^0 \Theta^0]} \leq 1.4. \end{cases}$$

The same assumption is made by Yuan and Zhang (2014) for analyzing the GCRF model with the ℓ_1 penalty and is also frequently used in compressed sensing. It is well known that this condition holds with high probability when X is sub-Gaussian with a well conditioned population covariance matrix satisfying certain regularity assumptions on the eigenvalues and n is sufficiently large, e.g., $n \geq O\big((p + s_0) \log(p + q)\big)$ (Candes and Tao, 2007; Yuan and Zhang, 2014).

The following lemma, which summarizes Proposition 3 from Yuan and Zhang (2014), ensures that $\beta(\Phi^0; r, \alpha)$ is positive for a GCRF model with

high probability when sample size n is large enough. That is, $\ell(\Phi)$ behaves like a strongly convex function locally in the cone $\|\Delta_{S_0^c}\|_1 \leq \alpha\|\Delta_{S_0}\|_1$, although $\ell(\Phi)$ is not a strongly convex function at Φ^0.

Lemma 2. *Let*

$$\begin{aligned}
\rho_1 &= 0.5\min\left(\lambda_{\max}(\Lambda^0)^{-1}\lambda_{\min}(\Sigma^0_{xx})\right), \quad \rho_2 = 1.5\lambda_{\max}(\Sigma^0_{xx}),\\
r_0 &= \min\left[0.5\lambda_{\min}(\Lambda^0),\ 0.13\sqrt{\lambda_{\max}[(\Theta^0)^T\Sigma^0_{xx}\Theta^0]/\rho_2}\right],\\
\beta_0 &= \left\{\frac{\rho_1}{40\lambda_{\max}(\Lambda^0)}\cdot\min\left[1, \frac{\lambda_{\min}(3\Lambda^0)}{16\lambda_{\max}\left((\Theta^0)^T\Sigma^0_{xx}\Theta^0\right)}\right]\right\}.
\end{aligned}$$

Assume that Assumption 1 holds with

$$s_0 = |S_0| + \lceil 4(\rho_2/\rho_1)\alpha^2|S_0|\rceil. \tag{3.11}$$

Then we have $\beta(\Phi^0; r, \alpha) \geq n\beta_0$ for $r \leq r_0$.

3.2 Rate of convergence for all points in HPD

We first show that for any point Φ in the HPD region, its error term $\Delta = \Phi - \Phi^0$ belongs to a cone, if $1/v_1$ is chosen properly.

Lemma 3. *If $1/v_1 > 2\|\ell(\Phi^0)\|_\infty$, then for any $\Phi = \Phi^0 + \Delta$ so that $L(\Phi) \leq L(\Phi^0)$, we have $\|\Delta_{S_0^c}\|_1 \leq \alpha\|\Delta_{S_0}\|_1$, where $\alpha = 1 + 2v_1/v_0$.*

We then show that all points from the HPD region, including the global maximum and all stationary points of the posterior distribution with

$L(\Phi) \leq L(\Phi^0)$, are close to the true parameter value within an optimal statistical precision. Our analysis allows the quantities (v_0, v_1, R) as well as the model size p, q and $|S_0|$ to grow with the sample size n, however, we suppress this dependence on n in our notation for convenience.

Theorem 1 (Rate of convergence for all points in HPD)**.** *Assume Assumption 1 holds with s_0 defined at (3.11). If*

(i) the prior hyper-parameters v_0, v_1 satisfy:

$$\frac{2\|\nabla \ell(\Phi^0)\|_\infty}{n} \leq \frac{1}{nv_1} = C_1\sqrt{\frac{\log(p+q)}{n}}, \quad \frac{1}{nv_0} = C_0\sqrt{\frac{\log(p+q)}{n}},$$

for some constants $C_0 \geq C_1$;

(ii) the matrix norm bound R satisfies $R < \frac{2\lambda_{\min}(\Lambda^0)\sqrt{r_0}}{\varepsilon_n}$;

(iii) the sample size n satisfies $n \geq \log(10(p+q)^2/\epsilon_0)$

then for any Φ from the HPD region (3.9), we have

$$\|\Phi - \Phi^0\|_F \leq \varepsilon_n := \frac{C_0 + C_1}{\beta_0}\sqrt{\frac{|S_0|\log(p+q)}{n}}$$

with probability no less than $1 - \epsilon_0$ where ϵ_0 is a constant from $(0, 1)$.

Our conditions and theoretical results require the following condition regarding the magnitude relationship among (p, q, n): $(p + s_0)\log(p + q) = o(n)$, to ensure that Assumption 1 holds with high probability and to ensure F-norm estimation error bound of Theorem 1 to go to zero. This is not a

restrictive requirement since our focus is high-dimensional settings where $\dim(X) = q \gg \dim(Y) = p$ and it still allows the covariate dimension q to be much larger than the sample size.

A proof of Theorem 1 is provided in the Supplementary Material. Our proof is motivated by Theorem 1 from Yuan and Zhang (2014). However, the proof technique in Yuan and Zhang (2014) is tailored to the Lasso penalty, which needs to be extended to handle our concave penalty function $\text{pen}_{\text{SS}}(\theta)$.

Theorem 1 does not impose any conditions on the mixing weight η and the difference between the two scale parameter v_0 and v_1, therefore Theorem 1 includes special cases such as $\eta = 0$, or $\eta = 1$, or $v_1 = v_0$. In the aforementioned special cases, the spike and slab Lasso penalty degenerates to the ordinary Lasso penalty with one unique global optimum. For Lasso penalty, Yuan and Zhang (2014) established a similar error bound for the global optimum, while our result is stronger since it establishes the error bound for all points in HPD including the global optimum.

3.3 Faster rate of convergence for a local optimum and its sparsistency

The result in Section 3.2 is for all points in the HPD region. Next we provide stronger results for estimation and selection accuracy for at least one local optimum in HPD.

Theorem 2 (Rate of convergence in ℓ_∞ norm and sparsistency)**.** *Assume Assumption 1 holds with s_0 defined at (3.11). Then, there exists a stationary point $\tilde{\Phi}$ in HPD such that*

$$\tilde{\Phi}_{S_0^c} = 0, \quad \|\tilde{\Phi} - \Phi^0\|_\infty \le r_n := 4c_H(C_1 + C_0)\sqrt{\frac{\log(p+q)}{n}}$$

with probability $1 - \epsilon_0$, if the following conditions hold:

(i) the prior hyper-parameters v_0, v_1, η satisfy: $0 < \eta \sim O(1) < 1$,

$$\frac{2\|\nabla \ell(\Phi^0)\|_\infty}{n} \le \frac{1}{nv_1} = C_1\sqrt{\frac{\log(p+q)}{n}}, \quad \frac{1}{nv_0} = C_0\sqrt{\frac{\log(p+q)}{n}},$$

for some constants $C_0 > C_1$;

(ii) $\theta^0_{\min} > r_n + \delta_0$ where $\delta_0 > [n\log(p+q)]^{-\alpha/2}$ with $0 < \alpha < 1$ and

$$r_n \le \min\left\{\frac{1}{3c_{\Sigma^0}d}, \frac{1}{3708d^2c^2_{\Gamma^0}c^4_{\Sigma^0}\rho_2}, \frac{c_{\Theta^0}}{2d}, \frac{2pen'_{SS}(0^+)}{n(c_H + 1/c_H)}\right\};$$

(iii) the sample size n satisfies $n \ge \log(10(p+q)^2/\epsilon_0)$.

The condition, $\theta^0_{\min} > r_n + \delta_0$, is the usual beta-min condition meaning that the minimal signal strength in Φ_{S_0} should be bigger than the ℓ_∞ error

bound by a small margin δ_0, where δ_0 can go to zero at a rate slower than $[n \log(p+q)]^{-\alpha}$. Under the beta-min condition, Theorem 2 ensures that $\min_{(i,j)\in S_0} |\tilde{\Phi}_{ij}| \geq \delta_0$, and consequently we have $\tilde{\Phi}$ achieve sparsistency, i.e., $\tilde{\Phi}_{S_0^c} = 0$ and $\tilde{\Phi}_{S_0} \neq 0$.

Different from Theorem 1, Theorem 2 requires η to be strictly between 0 and 1 and v_1 strictly bigger than v_0, so the ordinary one component Laplace prior, i.e., Lasso penalty, will not satisfy the assumptions here. Note that our theoretical results do not require η to be small and decrease to zero with the dimension nor allow v_1/v_0 to diverge, which seem to contradict to prior results on Bayesian variable selection using spike and slab priors such as George and McCulloch (1993); Ishwaran and Rao (2005); Narisetty and He (2014); Castillo et al. (2015). The main reason for this difference is that these approaches consider the integrated posterior on all the models after integrating out the continuous model parameters due to which they require multiplicity adjustment for a large number of models. In contrast, since our theoretical analysis studies the posterior on the continuous model parameters directly, our conditions on the prior parameters v_1 and η do not have a direct correspondence with the previous choices. In particular, our theoretical results are under condition that v_1 is not much larger than v_0 because a larger gap between them would imply more non-convexity

of the negative log posterior, which will make it difficult to compute and theoretically study its stationary points.

A proof for Theorem 2 is provided in the Supplementary Material, which is motivated by similar results from Ravikumar et al. (2011); Wytock and Kolter (2013); Loh and Wainwright (2017); Gan et al. (2019). We start with a restricted optimization problem:

$$\min_{\Lambda \succ 0, \Phi_{S_0^c}=0} L(\Phi), \tag{3.12}$$

then show that there exists a solution $\tilde{\Phi}$ to (3.12) that satisfies $\|\tilde{\Phi} - \Phi^0\|_\infty \leq r_n$. The last and most important step is to prove that $\tilde{\Phi}$ is indeed a local minimizer of the objective function $L(\Phi)$ by showing that $L(\Phi) \geq L(\tilde{\Phi})$ for any Φ in a small neighborhood of $\tilde{\Phi}$.

Previously, under mutual incoherence conditions, Wytock and Kolter (2013) showed that the convergence rate in ℓ_∞ norm for the Gaussian conditional random field model with ℓ_1 penalty is of the same order as ours. However, their approach requires the restrictive mutual incoherence condition, i.e., $\|\|H_{S_0^c S_0}(H_{S_0 S_0})^{-1}\|\|_\infty < 1$, which our approach does not require. We illustrate that this condition can be easily violated through the following toy example. Consider a simple Markov chain Gaussian conditional

random field model in Figure 1(a), with

$$\Lambda^0 = \begin{bmatrix} 1 & \rho & 0 \\ \rho & 1 & \rho \\ 0 & \rho & 1 \end{bmatrix}, \quad \Theta^0 = \begin{bmatrix} \rho\beta & 0 & 0 \\ 0 & \rho\beta & 0 \\ 0 & 0 & \rho\beta \end{bmatrix}.$$

In Figure 1(b), we plot $|||H_{S_0^c S_0}(H_{S_0 S_0})^{-1}|||_\infty$ for five different choices of β. For each β, the mutual incoherence condition will be violated once ρ is larger than some threshold.

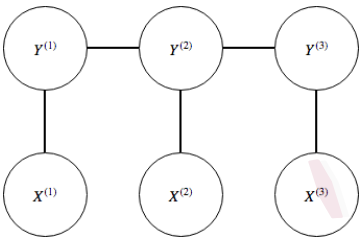

(a) Markov chain GCRF Model

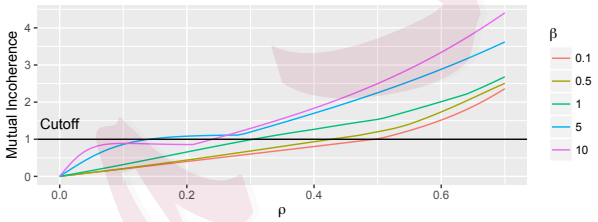

(b) Mutual incoherence is violated for large ρ

Figure 1: Violation of mutual incoherence condition for the chain graph.

3.4 On uniqueness of stationary points in HPD

While Theorem 2 asserts that there is one stationary point in the HPD region that has a desired rate of convergence, it is a natural question to ask if the stationary point is unique. Unfortunately, we cannot ascertain this directly for the posterior distribution using the spike and slab regularization.

On the other hand, if we consider a slightly modified version of the negative log-posterior minimization (2.6) given by

$$L_\kappa(\Theta) = -\ell(\Phi) + \kappa \text{Pen}(\Phi), \tag{3.13}$$

where κ is a parameter that enhances the amount of Bayesian regularization, the stationary solution can be proved to be unique for some choices of κ.

The modified objective function (3.13) can be viewed as the negative log-posterior corresponding to the fractional posterior distribution $\pi_\kappa(\Theta \mid \text{Data})$, which is the posterior distribution defined with respect to the likelihood of the data raised to power $1/\kappa$, i.e., $\pi_\kappa(\Theta \mid \text{Data}) \propto \exp(\ell(\Phi)/\kappa - \text{Pen}(\Phi))$. The HPD region corresponding this fractional posterior distribution can be defined accordingly as

$$\{\Phi : L_\kappa(\Phi) \leq L_\kappa(\Phi^0)\}. \tag{3.14}$$

Next we show that Theorem 1 and Theorem 2 can be extended to cover fractional posterior. In addition, we can show that with a proper choice of the hyper-parameters, the HPD region is uimodal with a unique stationary point that achieves the desired ℓ_∞ accuracy.

Theorem 3. *Assume Assumption 1 holds with s_0 defined at (3.11). Further assume the following conditions hold:*

(i) $\kappa = \log(p + q)$;

(ii) the prior hyper-parameters v_0, v_1, η *satisfy:* $0 < \eta \sim O(1) < 1$,

$$\frac{\|\nabla \ell(\Phi^0)\|_\infty}{n} \le \frac{\kappa}{nv_1} = C_1\sqrt{\frac{\log(p+q)}{n}}, \quad \frac{\kappa}{nv_0} = C_0\sqrt{\frac{\log(p+q)}{n}},$$

for some constants $C_0 > C_1$*;*

(iii) the matrix norm bound R *satisfies* $R < \frac{2\lambda_{\min}(\Lambda^0)\sqrt{r_0}}{\varepsilon_n}$*; and*

(iv) the sample size n *satisfies* $n \ge \log(10(p+q)^2/\epsilon_0)$*. Then with probability going to* 1*, any point from the HPD region* (3.14)*, we have*

$$\|\Phi - \Phi^0\|_F \le \varepsilon_n := \frac{C_0 + C_1}{\beta_0}\sqrt{\frac{|S_0|\log(p+q)}{n}}.$$

Further if we assume r_n *satisfies* $\theta^0_{\min} - r_n > \delta_0$ *where* $\delta_0 > [n\log(p+q)]^{-\alpha/2}$ *with* $0 < \alpha < 1$ *and*

$$r_n \le \min\left\{\frac{1}{3c_{\Sigma^0}d}, \frac{1}{3708d^2c^2_{\Gamma^0}c^4_{\Sigma^0}\rho_2}, \frac{c_{\Theta^0}}{2d}, \frac{2pen'_{SS}(0^+)}{n(c_H + 1/c_H)}\right\},$$

then the unique stationary point $\tilde{\Phi}$ *from the HPD region satisfies*

$$\tilde{\Phi}_{S_0^c} = 0, \quad \|\tilde{\Phi} - \Phi^0\|_\infty \le r_n := 4c_H(C_1 + C_0)\sqrt{\frac{\log(p+q)}{n}}$$

with probability converging to 1*.*

4. Empirical results

4.1 Simulation studies

In the simulation studies, we compare different methods in terms of parameter estimation, structure recovery and prediction. Following the studies

from Yuan and Zhang (2014), we generate X from a zero-mean multivariate Gaussian distribution with a *dense* precision matrix $\Theta^0_{xx} = 0.5(J + I)$, where J is the matrix of ones, and generate Y given X from the Gaussian conditional random field model (2.1) with the true (Θ^0, Λ^0) generated as follows. The precision matrix Λ^0 is generated as a random graph similar to the set-up of the random graph in Peng et al. (2009). We first generate the entries in the precision matrix following the distribution of $S \times B \times U_1$, where $(S + 1)/2 \sim \mathsf{Bern}(0.5)$, $B \sim \mathsf{Bern}(0.1)$, $U_1 \sim \text{Uniform}(1, 2)$, and the three random variables are independent. We then rescale the non-zero elements to assure positive definiteness of Λ. Specifically, we first sum the absolute value of each row, and then divide each off-diagonal entry by 1.1 fold of it. We then average the rescaled matrix with its transpose to ensure symmetry. Finally, the diagonal entries are all set to be one. We consider the following forms of true Θ^0:

1. Model 1 (Random Graph): entries in Θ^0 are generated as $S \times B \times U_2$ where S and B are random variables as defined before, and independent of $U_2 \sim \text{Uniform}(0.5, 1)$.

2. Model 2 (Banded Model 1): for i-th row of Θ^0, the $((i-1)/\lfloor q/p \rfloor + 1)$-th element is generated from $S \times B \times U_2$. All other entries are zero.

3. Model 3 (Banded Model 2): the i-th row of Θ^0 is of probability 0.1

to be non-zero and probability 0.9 to be all zero; when the i-th row of the Θ^0 is non-zero, its entries are generated with the distribution of $S \times B \times U_2$, where $(S+1)/2 \sim \text{Bern}(0.5)$, $B \sim \text{Bern}(0.1)$, and $U_2 \sim \text{Uniform}(0.5, 1)$.

For each model, we fix the observation size $n = 100$ and dimension of the outcome vector $p = 50$, and take the covariate dimension q to be $(50, 100, 200, 500)$. Results are summarized based on 100 replications. We report three metrics to measure the estimation, selection and prediction accuracy of each method: *i*) for estimation accuracy, we use Frobenius norm distance (denoted as Fnorm); *ii*) for selection accuracy of structure recovery, we use MCC (Matthews correlation coefficient):

$$\text{MCC} = \frac{\text{TP} \times \text{TN} - \text{FP} \times \text{FN}}{\sqrt{(\text{TP}+\text{FP})(\text{TP}+\text{FN})(\text{TN}+\text{FP})(\text{TN}+\text{FN})}},$$

where TP, TN, FP, FN are true positives, true negatives, false positives and false negatives, respectively; *iii*) for prediction accuracy, we use the average MSE on an independently generated test data set of size 100. When interpreting the results, it may not be meaningful to compare results across different values of q as the level of sparsity in (Θ^0, Λ^0) and the magnitude of the signal in Λ change with q. We recommend comparing the results across different methods for the same value of q.

In the simulation studies, we compare our method, denoted as BayesCRF,

with the following alternative methods: 1) Gaussian conditional random field model with ℓ_1 regularization based on the implementation of Wytock and Kolter (2013), denoted as L1-GCRF; 2) a joint graphical Lasso (Friedman et al., 2008) for (X, Y), denoted as GLasso; 3) a covariate adjusted Graphical model proposed by Cai et al. (2012), denoted as CAPME. As CAPME does not directly estimate Θ, we first estimate B, the regression coefficient matrix, and then use the relationship given by (2.4) to recover Θ. We fix $v_0 = \sqrt{1/(n\log(p+q))}$, $v_1 = 3v_0$, and $\eta = 0.5$ for our BayesCRF method with $\alpha = 1$ corresponding to the complete posterior, and choose the tuning parameters for all the aforementioned alternatives using cross-validation as suggested in the respective papers.

The results for the banded Model 1 are provided in Table 1. The results for the other models are presented in the Supplementary Material due to space limitation but we comment on them here. We have the following conclusions from the results: 1) Our method BayesCRF has achieved the best performance for parameter estimation (based on Fnorm), support recovery (based on MCC), and prediction (based on Test Error) in most of the cases considered. These results can be attributed to the adaptiveness of the spike and slab Lasso penalty. 2) The performance of GLasso is not as desirable as that of BayesCRF, likely due to the accumulation of error in

estimating the structure of X which is not relevant to the parameters of the conditional random field model as discussed in Section 2. 3) CAPME has a poor performance in terms of MCC and Fnorm measures, since it is not designed to detect the conditional dependence structure of interest. However, it works well for prediction since prediction depends on B alone. 4) L1-GCRF performs worse than BayesCRF but it generally performs better than the other competing methods, although its test error is too large in the random graph setting with $q = 500$ and $n = 100$.

Table 1: Banded Model 1: Performance comparison of different methods. Larger values of MCC indicate better performance while smaller values of Fnorm and Test Error indicate better performance. Best performing method is highlighted in boldface.

	$n = 100, q = 50, p = 50$			$n = 100, q = 100, p = 50$		
	MCC	Fnorm	Test Error	MCC	Fnorm	Test Error
GLasso	0.330(0.022)	4.223(0.040)	1.279(0.032)	0.314(0.015)	5.316(0.035)	1.390(0.035)
CAPME	-0.037(0.001)	30.346(2.709)	1.455(0.046)	-0.036(0.012)	43.642(3.320)	1.696(0.046)
L1-GCRF	0.130(0.020)	3.050(0.110)	**1.250(0.028)**	0.216(0.021)	3.595(0.194)	**1.309(0.031)**
BayesCRF	**0.409(0.026)**	**2.498(0.094)**	1.278(0.032)	**0.452(0.024)**	**2.453(0.077)**	1.335(0.031)
	$n = 100, q = 200, p = 50$			$n = 100, q = 500, p = 50$		
	MCC	Fnorm	Test Error	MCC	Fnorm	Test Error
GLasso	0.394(0.012)	9.118(0.015)	2.051(0.053)	0.304(0.046)	12.684(0.162)	2.777(0.187)
CAPME	-0.033(0.010)	63.073(6.914)	2.294(0.069)	0.071(0.004)	13.735(1.546)	2.232(0.060)
L1-GCRF	0.361(0.015)	5.369(0.228)	1.489(0.031)	0.412(0.011)	8.628(0.333)	1.665(0.041)
BayesCRF	**0.606(0.015)**	**3.163(0.110)**	**1.431(0.032)**	**0.674(0.011)**	**6.297(0.143)**	**1.555(0.035)**

4.2 Application: asset returns prediction

We now compare the performance of our method with the other alternatives for the problem of predicting asset returns. The dataset we consider is the weekly price data of S&P 500 stocks for 265 consecutive weeks from March 10, 2003 to March, 24, 2008 collected by Pfaff (2016). We screen out all the stocks with extremely low or high marginal variance and keep 67 stocks that vary modestly, i.e., stocks with a variance between 25 and 40. All the stock prices are log transformed. Let $Y_t = [Y_t^1, ..., Y_t^{67}] \in \mathbb{R}^{67}$ denote the stocks prices at time point t and $X_t = [Y_{t-5}, Y_{t-4}, Y_{t-3}, Y_{t-2}, Y_{t-1}]$ denote the prices for the previous five weeks. We want to recover the dependence structure between Y_t and X_t, and within Y_t, which will provide insights on the dependency between the prices of different stocks and between their previous prices. We will also measure how well we can predict Y_t using X_t since we cannot directly evaluate the quality of the estimated structure.

We apply all the methods on the first 212 days to estimate Φ and make predictions on the remaining 53 days using equation (2.4). We first standardize all the variables to have zero mean and unit variance. We then transform the data back to the original log-scale to make predictions. Tuning parameters for all the methods are selected from 5-fold cross-validation

and the average prediction errors are evaluated by:

$$\overline{Err} = \frac{1}{49} \sum_{t=213}^{265} ||Y_t - \hat{Y}_t||_2.$$

The average prediction errors for all the methods are provided in Table 2. BayesCRF achieves the smallest average prediction error. The prediction performance of Glasso and CAPME are similar, while the algorithm for L1-GCRF fails in making an accurate prediction.

The conditional graphs estimated from all the methods are shown in Figure 2. We observe the following: 1) BayesCRF detects that some of the concurrent prices of assets are conditionally dependent with each other (shown in the estimated Λ matrix), and there is an $AR(2)$-like structure for each asset across time (shown in estimated Θ), i.e., Y_t^i is conditionally dependent with Y_{t-1}^i, Y_{t-2}^i. Glasso and L1-GCRF detect much noisier patterns with longer time dependences. 2) BayesCRF provides sparser estimates of the matrices (Θ, Λ), and at the same time, its prediction accuracy is also the best. It suggests that BayesCRF provides desirable estimation with both sparsity and accuracy. In practice, it is favorable to have sparser estimates since sparse models reduce the cost of data processing and management.

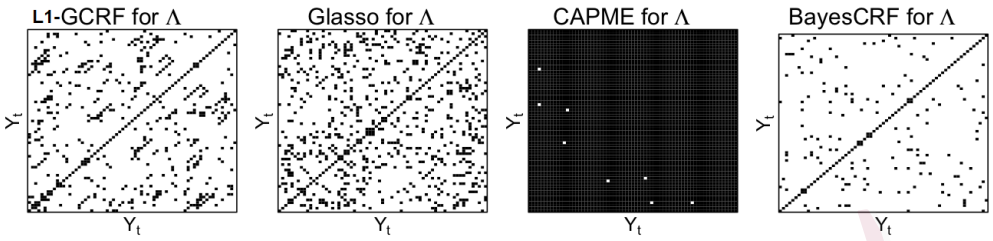

(a) Estimates for the precision matrix Λ for the asset return data.

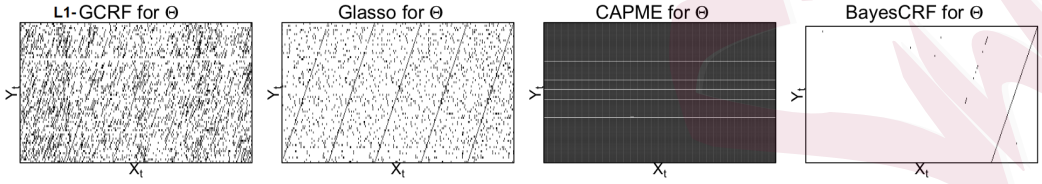

(b) Estimates for Θ for the asset return data. The i-th horizontal axis tick (from left to right) represents the i-th entry X_t and the i-th vertical axis tick (from down to top) represents the i-th entry Y_t.

Figure 2: Estimates of the graphs in the asset returns application. White represents the noise and black represents the selected signal.

Supplementary Material

Supplementary Material provides details regarding the properties of the proposed Bayesian regularization function, log likelihood function, our proposed EM algorithm for computations and its derivation, proofs for all the technical results, and additional simulation results.

Table 2: Average Prediction Error for Asset Return Prediction

BayesCRF	L1-GCRF	CAPME	Glasso
0.910(0.384)	3.817(0.468)	1.443(0.442)	1.250(0.495)

References

Banerjee, O., El Ghaoui, L., and d'Aspremont, A. (2008). Model selection through sparse maximum likelihood estimation for multivariate Gaussian or binary data. *The J. Mach. Learn. Res.*, 9:485–516.

Bickel, P. J. and Levina, E. (2008). Covariance regularization by thresholding. *Ann. Stat.*, 36(6):2577–2604.

Cai, T., Liu, W., and Luo, X. (2011). A constrained ℓ_1 minimization approach to sparse precision matrix estimation. *J. Amer. Statist. Assoc.*, 106(494):594–607.

Cai, T. T., Li, H., Liu, W., and Xie, J. (2012). Covariate-adjusted precision matrix estimation with an application in genetical genomics. *Biometrika*, 100(1):139–156.

Candes, E. and Tao, T. (2007). The Dantzig selector: Statistical estimation when p is much larger than n. *Ann. Stat.*, 35(6):2313–2351.

Castillo, I., Schmidt-Hieber, J., and Van der Vaart, A. (2015). Bayesian linear regression with sparse priors. *Ann. Stat.*, 43(5):1986–2018.

Deshpande, S. K., Ročková, V., and George, E. I. (2017). Simultaneous variable and covariance selection with the multivariate spike-and-slab lasso. *arXiv preprint arXiv:1708.08911*.

Fan, J. and Li, R. (2001). Variable selection via nonconcave penalized likelihood and its oracle properties. *J. Amer. Statist. Assoc.*, 96(456):1348–1360.

Friedman, J., Hastie, T., and Tibshirani, R. (2008). Sparse inverse covariance estimation with the graphical lasso. *Biostatistics*, 9(3):432–441.

Frot, B., Jostins, L., and McVean, G. (2019). Graphical model selection for Gaussian conditional random fields in the presence of latent variables. *J. Amer. Statist. Assoc.*, 114(526):723–734.

Gan, L., Narisetty, N. N., and Liang, F. (2019). Bayesian regularization for graphical models with unequal shrinkage. *J. Amer. Statist. Assoc.*, 114(527):1218–1231.

George, E. I. and McCulloch, R. E. (1993). Variable selection via Gibbs sampling. *J. Amer. Statist. Assoc.*, 88(423):881–889.

Ishwaran, H. and Rao, J. S. (2005). Spike and slab variable selection: Frequentist and Bayesian strategies. *Ann. Stat.*, 33(2):730–773.

Lafferty, J., McCallum, A., Pereira, F., et al. (2001). Conditional random fields: Probabilistic models for segmenting and labeling sequence data. In *Proceedings of the eighteenth international conference on machine learning, ICML*, volume 1, pages 282–289.

Lam, C. and Fan, J. (2009). Sparsistency and rates of convergence in large covariance matrix estimation. *Ann. Stat.*, 37(6B):4254–4278.

Loh, P.-L. and Wainwright, M. J. (2015). Regularized M-estimators with nonconvexity: Statistical and algorithmic theory for local optima. *J. Mach. Learn. Res.*, 16:559–616.

Loh, P.-L. and Wainwright, M. J. (2017). Support recovery without incoherence: A case for nonconvex regularization. *Ann. Stat.*, 45(6):2455–2482.

Meinshausen, N. and Bühlmann, P. (2006). High-dimensional graphs and variable selection with the lasso. *Ann. Stat.*, 34(3):1436–1462.

Narisetty, N. N. and He, X. (2014). Bayesian variable selection with shrinking and diffusing priors. *Ann. Stat.*, 42(2):789–817.

Negahban, S., Yu, B., Wainwright, M. J., and Ravikumar, P. K. (2009).

A unified framework for high-dimensional analysis of M-estimators with decomposable regularizers. In *NIPS*, pages 1348–1356.

Park, T. and Casella, G. (2008). The Bayesian lasso. *J. Amer. Statist. Assoc.*, 103(482):681–686.

Peng, J., Wang, P., Zhou, N., and Zhu, J. (2009). Partial correlation estimation by joint sparse regression models. *J. Amer. Statist. Assoc.*, 104(486):735–746.

Pfaff, B. (2016). *Financial Risk Modelling and Portfolio Optimisation with R*. John Wiley & Sons, Ltd, London, 2nd edition.

Ravikumar, P., Wainwright, M. J., Raskutti, G., and Yu, B. (2011). High-dimensional covariance estimation by minimizing ℓ_1-penalized log-determinant divergence. *Electronic Journal of Statistics*, 5:935–980.

Ročková, V. (2018). Bayesian estimation of sparse signals with a continuous spike-and-slab prior. *Ann. Stat.*, 46(1):401–437.

Ročková, V. and George, E. I. (2014). EMVS: The EM approach to Bayesian variable selection. *J. Amer. Statist. Assoc.*, 109(506):828–846.

Ročková, V. and George, E. I. (2016). Fast Bayesian factor analysis via

automatic rotations to sparsity. *J. Amer. Statist. Assoc.*, 111(516):1608–1622.

Ročková, V. and George, E. I. (2018). The spike-and-slab lasso. *J. Amer. Statist. Assoc.*, 113(521):431–444.

Rothman, A. J., Levina, E., and Zhu, J. (2010). Sparse multivariate regression with covariance estimation. *Journal of Computational and Graphical Statistics*, 19(4):947–962.

Sohn, K.-A. and Kim, S. (2012). Joint estimation of structured sparsity and output structure in multiple-output regression via inverse-covariance regularization. In *AISTATS*, pages 1081–1089.

Tibshirani, R. (1996). Regression shrinkage and selection via the lasso. *J. Royal Stat. Soc. B*, 58(1):267–288.

Witten, D. and Tibshirani, R. (2009). Covariance-regularized regression and classification for high-dimensional problems. *J. Royal Stat. Soc. B*, 71(3):615–636.

Wytock, M. and Kolter, Z. (2013). Sparse Gaussian conditional random fields: Algorithms, theory, and application to energy forecasting. In *ICML-13*, pages 1265–1273.

Yin, J. and Li, H. (2011). A sparse conditional Gaussian graphical model for analysis of genetical genomics data. *The Annals of Applied Statistics*, 5(4):2630.

Yuan, X.-T. and Zhang, T. (2014). Partial Gaussian graphical model estimation. *IEEE Transactions on Information Theory*, 60(3):1673–1687.

Zhang, C.-H. (2010). Nearly unbiased variable selection under minimax concave penalty. *Ann. Stat.*, 38(2):894–942.

Zhang, C.-H. and Zhang, T. (2012). A general theory of concave regularization for high-dimensional sparse estimation problems. *Statistical Science*, 27(4):576–593.